0090-9556/10/3807-1211–1217$20.00
DRUG METABOLISM AND DISPOSITION
Vol. 38, No. 7
31625/3591857
Printed in U.S.A.

DMD 38:1211–1217, 2010

Role of UDP-Glucuronosyltransferase Isoforms in 13-*cis* Retinoic Acid Metabolism in Humans

Sophie E. Rowbotham, Nicola A. Illingworth, Ann K. Daly, Gareth J. Veal, and Alan V. Boddy

Northern Institute for Cancer Research (S.E.R., N.A.I., G.J.V., A.V.B.); and Institute of Cellular Medicine, Newcastle University Medical School, Newcastle upon Tyne, United Kingdom (A.K.D.)

Received December 14, 2009; accepted March 19, 2010

ABSTRACT:

13-*cis* Retinoic acid (13*cis*RA, isotretinoin) is an important drug in both dermatology, and the treatment of high-risk neuroblastoma. 13*cis*RA is known to undergo cytochrome P450-mediated oxidation, mainly by CYP2C8, but phase II metabolic pathways have not been characterized. In the present study, the glucuronidation activities of human liver (HLM) and intestinal microsomes (HIM), as well as a panel of human UDP-glucuronosyltransferases (UGTs) toward both 13*cis*RA and the 4-oxo metabolite, 4-oxo 13*cis*RA, were compared using high-performance liquid chromatography. Both HLM and, to a greater extent, HIM catalyzed the glucuronidation of 13*cis*RA and 4-oxo 13*cis*RA. Based on the structures of 13*cis*RA and 4-oxo 13*cis*RA, the glucuronides formed are conjugated at the terminal carboxylic acid. Further analysis revealed that UGT1A1, UGT1A3, UGT1A7, UGT1A8, and UGT1A9 were the major isoforms responsible for the glucuronidation of both substrates. For 13*cis*RA, a pronounced substrate inhibition was observed with individual UGTs and with HIM. UGT1A3 exhibited the highest rate of activity toward both substrates, and a high rate of activity toward 13*cis*RA glucuronidation was also observed with UGT1A7. However, for both substrates, K_m values were above concentrations reported in clinical studies. Therefore, UGT1A9 is likely to be the most important enzyme in the glucuronidation of both substrates as this enzyme had the lowest K_m and is expressed in both the intestine and at high levels in the liver.

Retinoids are derivatives of retinol (vitamin A) that regulate numerous biological processes, including embryogenesis, growth, differentiation, vision, and reproduction (Evans and Kaye, 1999). Retinoic acid is the main biologically active derivative of retinol and exists in several stereoisomeric forms, including all-*trans* retinoic acid (ATRA), 13-*cis* retinoic acid (13*cis*RA), and 9-*cis* retinoic acid. Retinoids exhibit several pharmacological properties useful in dermatology (Peck and DiGiovanna, 1994), as well as in cancer prevention and chemotherapy (Hong and Itri, 1994). The most dramatic clinical benefits with retinoids are observed with ATRA for the treatment of acute promyelocytic leukemia and 13*cis*RA in the treatment of high-risk neuroblastoma (Reynolds and Lemons, 2001; Matthay et al., 2009).

The oxidative metabolism of 13*cis*RA has been extensively examined and involves the cytochrome P450 (P450) enzyme system, a superfamily of heme-containing monooxygenases that have a central role in the oxidative metabolism of a variety of endogenous and exogenous compounds. As a result of P450-mediated metabolism, intermediates that may exert toxicity or carcinogenicity are formed. Such intermediates are also targets for phase II drug metabolism, which renders them inactive, with the polar products subsequently excreted via the kidneys. Several P450s can catalyze the oxidation of 13*cis*RA, including P450s 3A7, 2C8, 4A11, 1B1, 2B6, 2C9, 2C19, and 3A4 (Chen et al., 2000; Marill et al., 2002). The major metabolites formed after P450-mediated oxidation are 4-hydroxy 13*cis*RA and 4-oxo 13*cis*RA.

ATRA and its oxidized metabolites undergo glucuronidation catalyzed by UDP-glucuronosyltransferases (UGTs) in animals and humans. The UGTs catalyze the transfer of the glucuronic acid moiety from the cofactor UDP-glucuronic acid to the substrate, resulting in a metabolite with greater polarity and water solubility. The human UGTs 1A8 and 2B7 have been identified as being responsible for the glucuronidation of ATRA, 4-oxo ATRA, 4-hydroxy ATRA, and 5,6-epoxy ATRA (Cheng et al., 1999; Czernik et al., 2000; Samokyszyn et al., 2000). Analysis of the glucuronidation products revealed that ATRA, 4-oxo ATRA, and 5,6-epoxy ATRA formed carboxyl-linked glucuronides, whereas 4-hydroxy ATRA was glucuronidated at its hydroxyl group (Samokyszyn et al., 2000). In view of its strong homology with ATRA, it is probable that 13*cis*RA also undergoes glucuronidation.

To date, 21 functional UGT isoforms have been identified in humans (http://www.ugtalleles.ulaval.ca), many of which catalyze the glucuronidation of a wide variety of environmental carcinogens, dietary chemopreventatives, and anticancer agents (Nagar and Remmel, 2006). However, no studies examining the glucuronidation of 13*cis*RA have as yet been reported. In the present study the activities and kinetics of human liver and intestinal microsomes as well as a panel of recombinant human UGTs were determined to identify those likely to be responsible for 13*cis*RA and 4-oxo 13*cis*RA glucuronidation in humans.

Materials and Methods

Materials. 13-*cis* Retinoic acid, all-*trans* retinoic acid, and β-glucuronidase (from *Helix pomatia*) were purchased from Sigma-Aldrich (Poole, UK). 4-Oxo

This work was supported by Cancer Research UK.

Article, publication date, and citation information can be found at http://dmd.aspetjournals.org.

doi:10.1124/dmd.109.031625.

ABBREVIATIONS: ATRA, all-*trans* retinoic acid; 13*cis*RA, 13-*cis* retinoic acid; P450, cytochrome P450; UGT, UDP-glucuronosyltransferase; HPLC, high-performance liquid chromatography; HLM, human liver microsomes; HIM, human intestinal microsomes; UDPGA, UDP-glucuronic acid.

13-*cis* retinoic acid (Ro 22-6595) and 4-oxo all-*trans* retinoic acid (Ro 12-4824) were generously provided by F. Hoffmann-La Roche (Basel, Switzerland). UGT Reaction Mix Solution A (25 mM UDP) and UGT Reaction Mix Solution B (250 mM Tris · HCl, 40 mM $MgCl_2$, and 0.125 mg/ml alamethicin) were purchased from BD Gentest (Oxford, UK). Pooled human liver and intestinal microsomes as well as Supersomes expressing the recombinant human UGT1A1, UGT1A3, UGT1A4, UGT1A6, UGT1A7, UGT1A8, UGT1A9, UGT1A10, UGT2B4, UGT2B7, UGT2B15, and UGT2B17 enzymes were also purchased from BD Gentest. In addition, control microsomes with wild-type baculovirus were obtained. High-performance liquid chromatography (HPLC)-grade acetonitrile and glacial acetic acid were obtained from Thermo Fisher Scientific (Loughborough, UK).

Characterization of 13*cis*RA and 4-Oxo 13*cis*RA Glucuronidation. Glucuronidation activity was determined in pooled human liver microsomes

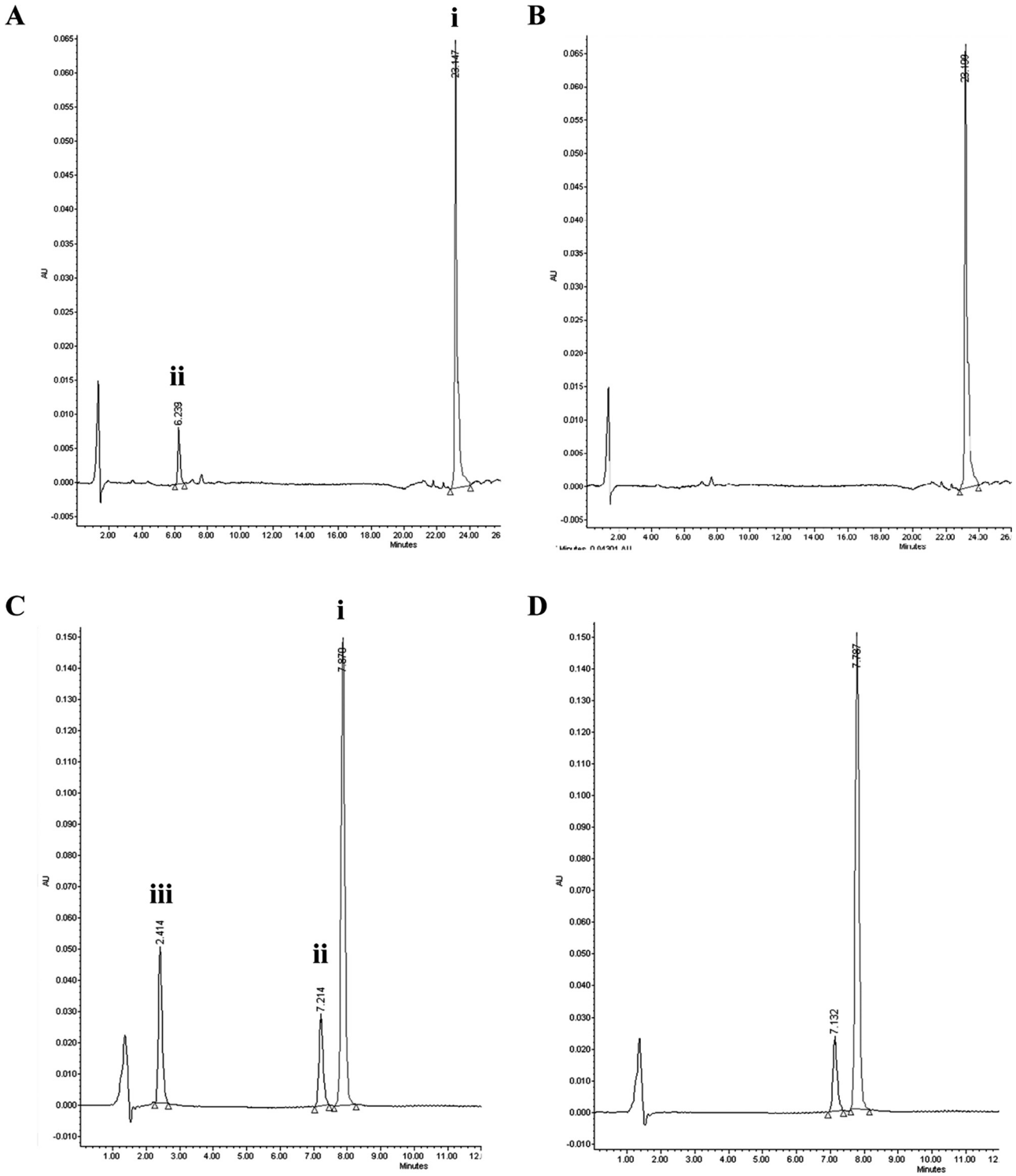

FIG. 1. Representative HPLC chromatograms illustrating the in vitro glucuronidation of 13*cis*RA and 4-oxo 13*cis*RA by UGT1A3. Absorbance units are measured on the *y*-axis, and time in minutes is measured on the *x*-axis. A, 13*cis*RA glucuronidation. 13*cis*RA (i) eluted at 23.1 min and 13*cis*RA glucuronide (ii) at 6.2 min. B, HPLC chromatogram of the same incubation shown in A, after treatment with β-glucuronidase. C, 4-oxo 13*cis*RA glucuronidation. 4-Oxo 13*cis*RA (i) eluted at 7.9 min, 4-oxo ATRA (ii) at 7.2 min, and 4-oxo 13*cis*RA glucuronide (iii) at 2.4 min. D, HPLC chromatogram of the same incubation shown in C, after treatment with β-glucuronidase.

(HLM), human intestinal microsomes (HIM), and Supersomes containing different cDNA-expressed UGT isoforms (UGT1A1, UGT1A3, UGT1A4, UGT1A6, UGT1A7, UGT1A8, UGT1A9, UGT1A10, UGT2B4, UGT2B7, UGT2B15, and UGT2B17). Conditions for linearity with respect to time and protein concentration were optimized in preliminary studies. The incubation mixture consisted of enzyme fractions (0.5 mg/ml total protein), 13*cis*RA (100 μM), or 4-oxo 13*cis*RA (100 μM), alamethicin (25 μg/ml), $MgCl_2$ (8 mM), UDPGA (2 mM), and methanol (0.25%) made up to a final volume (200 μl) with Tris-HCl buffer (50 mM, pH 7.5). Incubations were performed in a shaking water bath at 37°C for 60 min. Reactions were initiated by the addition of enzyme and terminated with ice-cold acetonitrile (400 μl). Incubations conducted with control Supersomes served as a negative control. Samples were vortex mixed and centrifuged at 17,900*g* for 5 min. Supernatant (200 μl) was removed and evaporated to dryness, and the residue was reconstituted in 200 μl of 0.1% glacial acetic acid, pH 5.0, before HPLC analysis. All incubations were performed in triplicate.

Hydrolysis of 13*cis*RA and 4-oxo 13*cis*RA Glucuronides. To samples prepared from the incubations as described above, β-glucuronidase (80 units) in potassium phosphate buffer (75 mM, pH 6.8) was added. The mixture was incubated in a shaking water bath at 37°C for 30 min. Reactions were terminated by the addition of ice-cold acetonitrile (400 μl). Control incubations were prepared under the same conditions, but with the addition of β-glucuronidase after the acetonitrile. Samples were vortex mixed and centrifuged at 17,900*g* for 5 min. Supernatant (200 μl) was removed and evaporated to dryness. Residue was reconstituted in 200 μl of 0.1% glacial acetic acid, pH 5.0, before HPLC analysis. All reactions were performed in triplicate.

HPLC Analysis. Analysis of 13*cis*RA and 13*cis*RA glucuronide was performed using a 2695 Separations Module and a 996 Photodiode Array UV Detector with Empower 2 software for data acquisition and analysis (Waters, Milford, MA). The UV detector was set to monitor 200 to 400 nm, isolating at 374 nm. Separation was performed on a Luna C18 (2) column (50 × 2.0 mm, 3 μm) (Phenomenex, Torrance, CA) by gradient reverse-phase chromatography. The mobile phase consisted of 0.1% glacial acetic acid, pH 5.0 (A) and 100% acetonitrile (B). Analysis was performed at a constant flow rate of 0.2 ml/min and an injection volume of 20 μl, and the gradient ran from 60% A to 60% B between 0 and 2 min. It remained at 60% B for 2 min and then switched back to 60% A between 4 and 5 min, remaining at 60% A for 10 min before switching to 100% B between 15 and 16 min. It remained at 100% B for 10 min and finally switched back to 60% A between 26 and 30 min, remaining at 60% A until 40 min. Analysis of 4-oxo 13*cis*RA and 4-oxo 13*cis*RA glucuronide was performed as described above, but with an alternative gradient, running from 60% A to 60% B between 0 and 2 min and remaining at 60% B for 2 min before switching back to 60% A between 4 and 5 min, where it remained until 20 min. The 13*cis*RA and 4-oxo 13*cis*RA glucuronide peaks were identified by treating the metabolites with β-glucuronidase, which hydrolyzes the glucuronide back to the aglycone. Analysis of 13*cis*RA and 4-oxo 13*cis*RA glucuronides was considered to be semiquantitative, because authentic standards were not available.

Determination of Kinetic Parameters for 13*cis*RA and 4-oxo 13*cis*RA Glucuronide Formation. Kinetic parameters for 13*cis*RA and 4-oxo 13*cis*RA glucuronide formation were determined using HLM and HIM, as well as UGT1A1, UGT1A3, UGT1A7, UGT1A8, and UGT1A9 Supersomes. All incubations were performed as described above. 13*cis*RA concentrations ranged from 0 to 250 μM, and 4-oxo 13*cis*RA concentrations ranged from 0 to 100 μM. There was an upper limit on the 4-oxo 13*cis*RA due to the concentration of the stock solution in ethanol. Substrate concentration and velocity data for 13*cis*RA and 4-oxo 13*cis*RA glucuronidation were fitted by the hyperbolic Michaelis-Menten model (eq. 1); for data exhibiting atypical kinetics, a substrate inhibition model was fitted (eq. 2):

$$v = V_{max}[S]/K_m + [S] \quad (1)$$

$$v = V_{max}[S]/(K_m + [S](1 + [S]/K_i)) \quad (2)$$

where v is the rate of reaction, V_{max} is the maximum velocity estimate, $[S]$ is the substrate concentration, K_m is the Michaelis-Menten constant, and K_i is the substrate inhibition constant. Units of K_m and K_i are given in micromolar concentrations. Because authentic standards were unavailable for the 13*cis*RA and 4-oxo 13*cis*RA glucuronides, V_{max} units were given as the peak area generated, as determined by HPLC analysis, in microvolts per second per second. Nonlinear regression was performed with GraphPad Prism software (GraphPad Software Inc., San Diego, CA).

Results

Identification of 13*cis*RA and 4-Oxo 13*cis*RA Glucuronides. Incubation of 13*cis*RA with HLM, HIM, recombinant UGT isoforms, and UDPGA resulted in the appearance of a novel chromatographic peak that was visible using a HPLC UV method previously optimized for the detection of 13*cis*RA (Fig. 1A). The glucuronide peak had a shorter retention time (6.2 min) compared with that for 13*cis*RA (23.1 min), and the rate of generation of this peak was dependent on microsomal protein concentration and incubation time. After incubation of 4-oxo 13*cis*RA with HLM, HIM, recombinant UGT isoforms, and UDPGA, another novel chromatographic peak was visible using a HPLC UV method that had previously been optimized for the detection of 4-oxo 13*cis*RA (Fig. 1C). An additional substrate peak was also observed. This was identified as 4-oxo ATRA and was formed as a result of minor isomerization of 4-oxo 13*cis*RA. The glucuronide peak retention time was 2.4 min, compared with 7.9 min for 4-oxo 13*cis*RA and 7.2 min for 4-oxo ATRA; again, the peak area increased with microsomal protein and incubation time. Treatment of

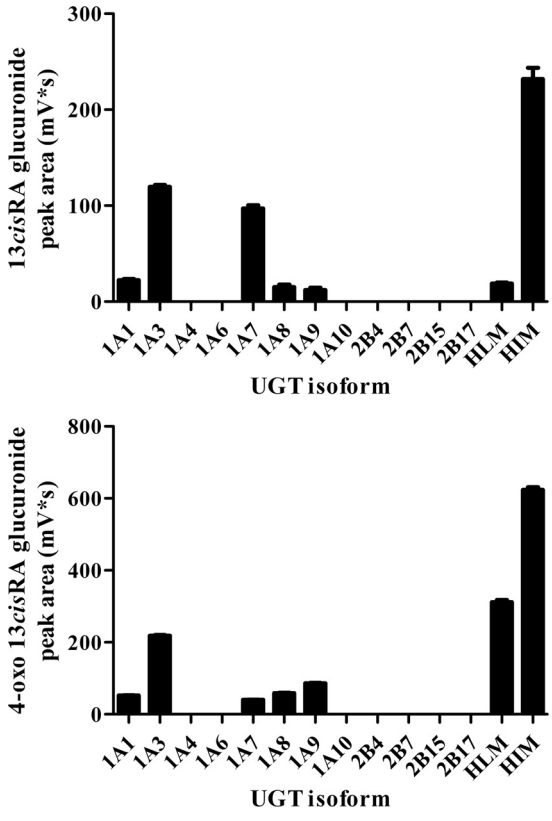

FIG. 2. 13*cis*RA and 4-oxo 13*cis*RA glucuronidation. Top, 13*cis*RA glucuronidation. Bottom, 4-oxo 13*cis*RA glucuronidation. Glucuronidation activity was determined in pooled human liver and intestinal microsomes and Supersomes containing different cDNA-expressed UGT isoforms (UGT1A1, UGT1A3, UGT1A4, UGT1A6, UGT1A7, UGT1A8, UGT1A9, UGT1A10, UGT2B4, UGT2B7, UGT2B15, and UGT2B17). Data are shown as the mean ± S.E.M.; $n = 3$. Incubation conditions were 60 min at 37°C with 0.5 mg/ml protein, and assays were performed in triplicate.

both incubates with β-glucuronidase resulted in complete disappearance of the metabolite peaks, indicating that the metabolites are glucuronide conjugates of 13*cis*RA and 4-oxo 13*cis*RA, respectively (Fig. 1, B and D).

Characterization of 13*cis*RA and 4-Oxo 13*cis*RA Glucuronidation. Screening of 13*cis*RA and 4-oxo 13*cis*RA glucuronosyltransferase activity was performed using HLM and HIM, as well as 12 recombinant UGT isoforms (UGT1A1, UGT1A3, UGT1A4, UGT1A6, UGT1A7, UGT1A8, UGT1A9, UGT1A10, UGT2B4, UGT2B7, UGT2B15, and UGT2B17). HLM, HIM, UGT1A1, UGT1A3, UGT1A7, UGT1A8, and UGT1A9 were found to catalyze both 13*cis*RA and 4-oxo 13*cis*RA glucuronide formation (Fig. 2). UGT1A4, UGT1A6, UGT1A10, UGT2B4, UGT2B7, UGT2B15, and UGT2B17 exhibited no detectable catalytic activity toward either 13*cis*RA or 4-oxo 13*cis*RA under the incubation conditions used.

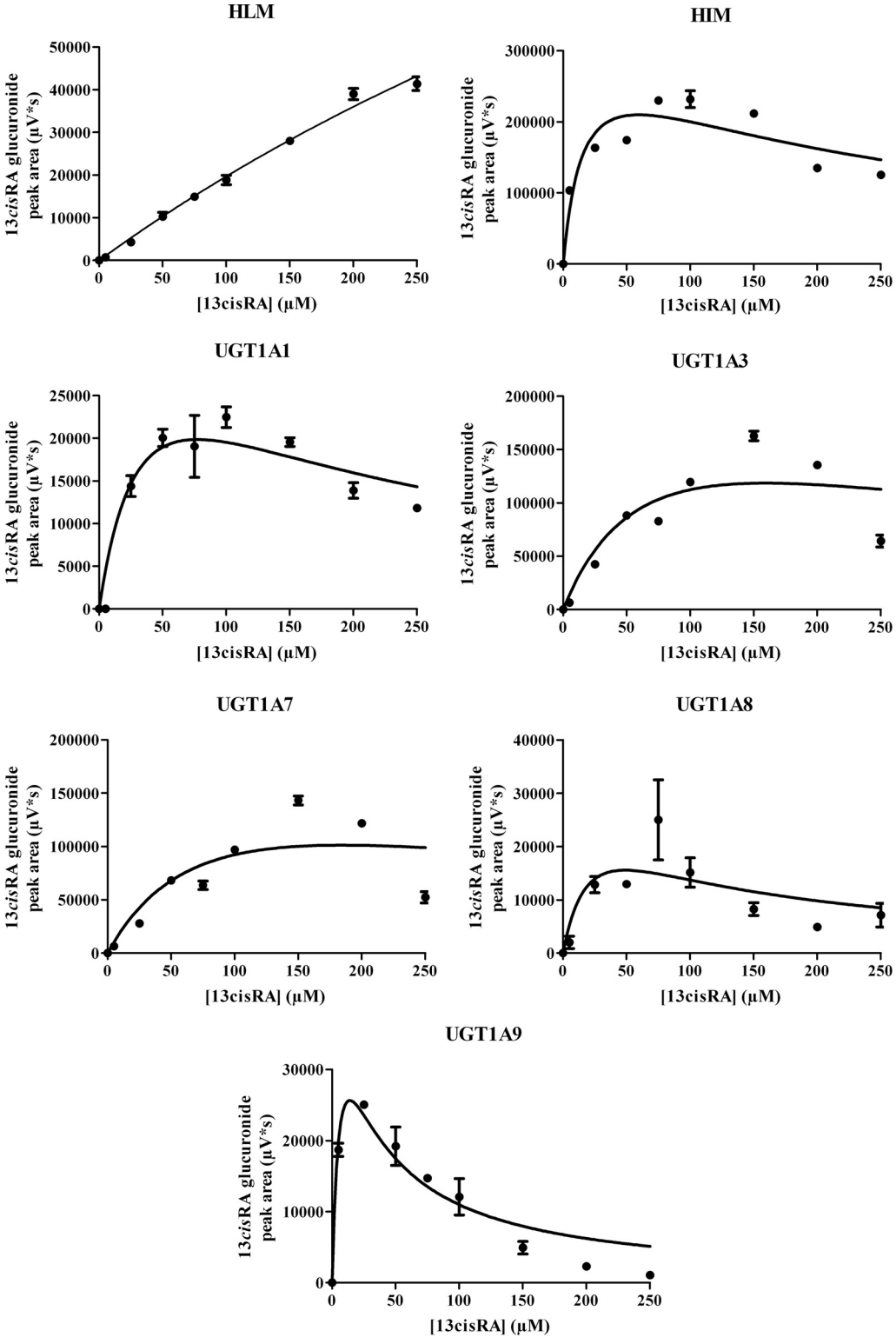

FIG. 3. Atypical kinetic profiles observed for 13*cis*RA glucuronide formation. Kinetic analysis was performed using pooled human liver and intestinal microsomes, as well as recombinant UGT1A1, UGT1A3, UGT1A7, UGT1A8, and UGT1A9 isoforms. Data are shown as the mean ± S.E.M.; $n = 3$. Incubations were performed in triplicate and carried out across a substrate concentration range of 0 to 250 μM.

TABLE 1

Kinetic parameter estimates for the formation of 13cisRA and 4-oxo 13cisRA glucuronides in human liver and intestinal microsomes and recombinant UGT isoforms

Data are expressed as means ± S.E.M.; n =3.

UGT Protein Source	4-Oxo 13*cis*RA			13*cis*RA			
	V_{max}	K_m	Goodness of Fit (r^2)	V_{max}	K_m	K_i	Goodness of Fit (r^2)
	$\mu V \cdot s/s$	μM		$\mu V \cdot s/s$	μM		
HLM	199 ± 70	95 ± 58	0.88	59 ± 17	974 ± 342	N.A.	0.99
HIM	304 ± 30	69 ± 14	0.98	1120 ± 800	200 ± 98	18 ± 9	0.85
UGT1A1	40 ± 4	175 ± 27	0.99	22[a]	78[a]	77[a]	0.86
UGT1A3	226 ± 50	266 ± 76	0.99	134[a]	161[a]	157[a]	0.78
UGT1A7	19 ± 3	51 ± 17	0.94	114[a]	186[a]	182[a]	0.73
UGT1A8	24 ± 2	36 ± 7	0.98	17[a]	49[a]	49[a]	0.50
UGT1A9	30 ± 1	18 ± 3	0.98	29[a]	14[a]	14[a]	0.88

N.A., not applicable.
[a] Precise estimates of the parameters could not be determined.

Determination of Kinetic Parameters for 13*cis*RA and 4-Oxo 13*cis*RA Glucuronide Formation. Kinetic analyses of 13*cis*RA and 4-oxo 13*cis*RA glucuronide formation were performed using HLM, HIM, and recombinant UGT1A1, UGT1A3, UGT1A7, UGT1A8, and UGT1A9 isoforms. Both 13*cis*RA and 4-oxo 13*cis*RA glucuronides were formed in varying amounts and rates across all UGT sources studied. HIM, which comprised a pool of more than one UGT enzyme, had the highest rate of glucuronidation toward both substrates. The formation of the 13*cis*RA glucuronide exhibited atypical kinetics across all UGT sources (Fig. 3; Table 1), except HLM for which data were fitted by the hyperbolic Michaelis-Menten model. The V_{max} and K_m for HLM were 59 ± 17 $\mu V \cdot s/s$ and 974 ± 342 μM, respectively. For HIM and recombinant UGT isoforms, data were fitted by the substrate inhibition model. Although the model provided a reasonable fit to the data, estimation of the kinetic parameters was possible only for HIM, with V_{max}, K_m, and K_i values of 1116 ± 804 $\mu V \cdot s/s$, 200 ± 98 μM, and 18 ± 9 μM, respectively. Estimates of K_m and K_i for the individual UGTs were highly correlated and ranged from 14 μM for UGT1A9 to 186 μM for UGT1A7. For reference, reported plasma concentrations of 13*cis*RA in neuroblastoma patients are on average 3 to 5 μM and rarely exceed 10 μM (Veal et al., 2007). The range of concentrations of 4-oxo 13*cis*RA that could be used to characterize the kinetics of glucuronide formation was limited by the amount of substrate available and the maximum concentration of 4-oxo 13*cis*RA in the stock solution in ethanol. The available data (up to 100 μM) were fitted well by the hyperbolic Michaelis-Menten model (Fig. 4; Table 1). Values for V_{max} were 199 ± 70 and 304 ± 30 $\mu V \cdot s/s$ in HLM and HIM, respectively, with corresponding values of K_m being 95 ± 58 and 69 ± 14 μM. Upon comparing glucuronidation activities of individual isoforms, UGT1A3 had a higher V_{max} toward 4-oxo 13*cis*RA than the other isoforms examined. Estimates of K_m ranged from 18 μM for UGT1A9 to 266 μM for UGT1A3. Reported plasma concentrations for 4-oxo 13*cis*RA can be up to 10 μM on day 14 of administration, but on average are nearer 6 μM (Veal et al., 2007).

Discussion

An in vitro HPLC-based assay has been developed to characterize the generation of 13*cis*RA and 4-oxo 13*cis*RA glucuronides using HLM, HIM, and recombinant UGT isoforms. Positive identification of these metabolites as glucuronides was based on sensitivity to β-glucuronidase treatment, resulting in complete disappearance of the metabolite peaks generated. Both HLM and HIM were found to catalyze the glucuronidation of 13*cis*RA and 4-oxo 13*cis*RA, with the highest rate of activity toward both substrates seen for HIM. This result could be particularly significant for an orally administered drug such as 13*cis*RA. Further investigations revealed that UGT1A1, UGT1A3, UGT1A7, UGT1A8, and UGT1A9 were the major isoforms responsible for the glucuronidation of both substrates.

Enzyme kinetic studies were performed with microsomes from human liver and intestine and with human UGT isoforms UGT1A1, UGT1A3, UGT1A7, UGT1A8, and UGT1A9 for both substrates. Although only a limited range of concentrations of 4-oxo 13*cis*RA could be explored, the concentrations far exceeded those reported clinically. For the parent drug, all enzyme sources other than HLM showed evidence of substrate inhibition. Although it was not possible to determine the parameters of this phenomenon precisely, inspection of the kinetic plots and the estimated parameters suggests that for the majority of enzyme sources, atypical kinetics of glucuronidation is not clinically important. The exception to this is UGT1A9, which showed signs of substrate inhibition at 50 μM. Substrate inhibition kinetics have been reported for other UGT substrates, including resveratrol (Iwuchukwu and Nagar, 2010).

The kinetic profiles for 4-oxo 13*cis*RA glucuronidation by HLM, HIM, and all of the UGT isoforms studied followed Michaelis-Menten kinetics, allowing determination of apparent K_m and V_{max} values. The 4-oxo metabolite appeared to be a better substrate for glucuronidation in HLM, in that the V_{max} value was higher than that for the parent compound. However, it should be noted that the K_m values for both substrates were higher than the maximal plasma concentrations observed in patients (Veal et al., 2007). In addition, glucuronidation in the intestine may be more relevant as the rate of reaction was highest for HIM, particularly at concentrations typically achieved in plasma. The intestine may be exposed to higher concentrations during drug absorption, but the degree of substrate inhibition was not marked at concentrations less than 100 μM in enzyme sources other than UGT1A9.

Caution in the interpretation of the estimated parameters is necessary because, unlike P450s, UGTs do not have a measurable chromophore representative of active protein; therefore, the amount of active UGT in any given recombinant preparation is unknown, and activities are normalized to milligrams of total protein rather than picomoles of UGT. The inability to quantify UGT expression levels in recombinant systems makes it difficult to verify the relative importance of individual isoforms in a particular glucuronidation pathway in which multiple UGTs may be involved. One approach to overcome this problem is through implementation of the relative activity factor method. This method was first used to investigate P450-dependent activity (Crespi and Miller, 1999) and measures the activities of an enzyme-selective probe substrate in recombinant UGT enzymes and pooled HLM. However, because of the broad overlapping substrate specificity between the UGTs, one caveat with the rela-

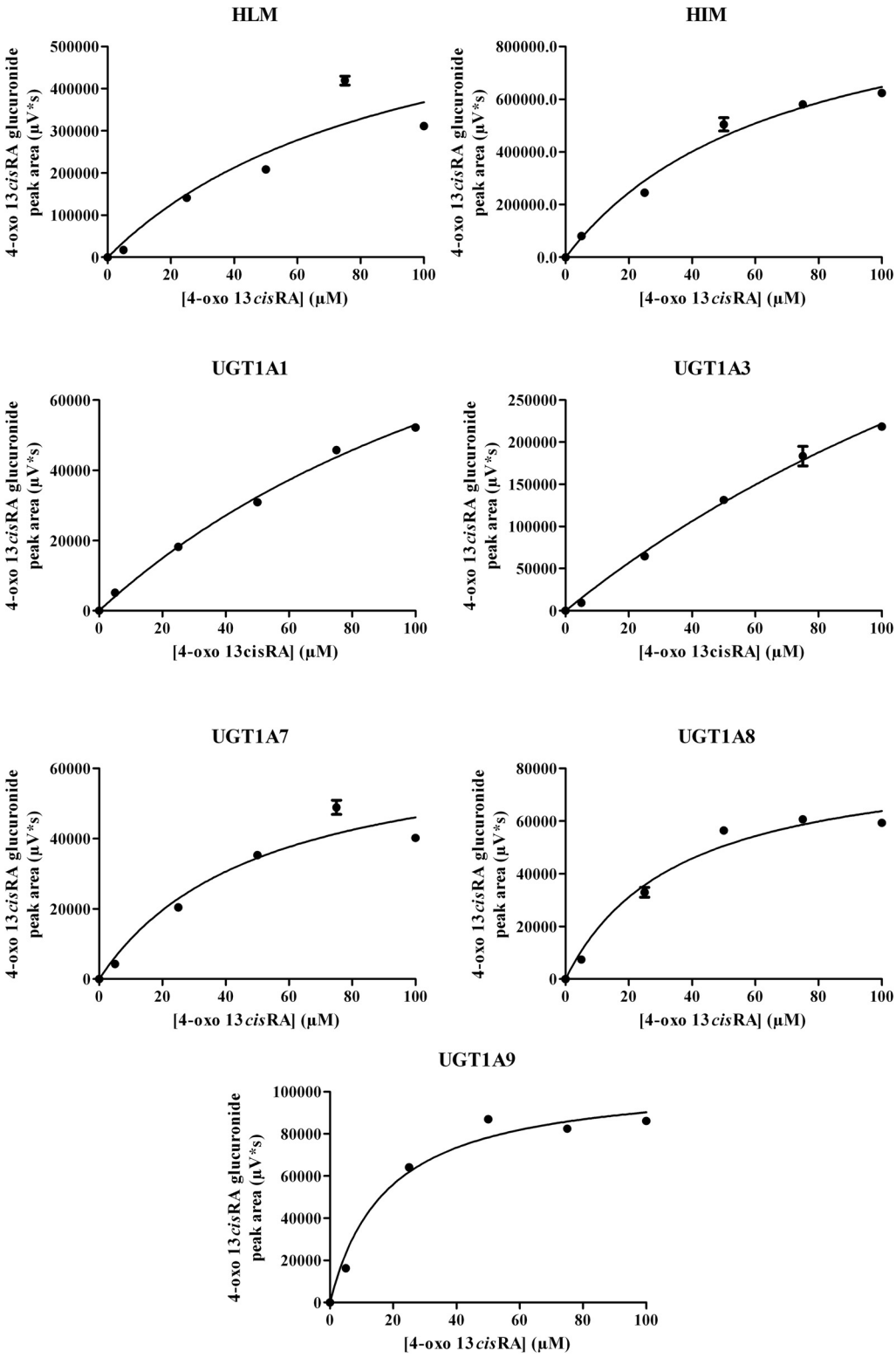

FIG. 4. Kinetic profiles observed for 4-oxo 13*cis*RA glucuronide formation. Kinetic analysis was performed using pooled human liver and intestinal microsomes, as well as recombinant UGT1A1, UGT1A3, UGT1A7, UGT1A8, and UGT1A9 isoforms. Data are shown as the mean ± S.E.M.; $n = 3$. Incubations were performed in triplicate and carried out across a substrate concentration range of 0 to 100 μM.

tive activity factor method for UGT reaction phenotyping is that probe substrates have not been identified for all of the major UGT isoforms.

Examination of the structures of 13*cis*RA and 4-oxo 13*cis*RA (Fig. 5) and comparison with the glucuronidation of ATRA allow tentative assignment of the position of glucuronidation. Because glucuronidation requires either a –COOH, –OH, $–NH_2$, or –SH functional group for conjugation with α-D-glucuronic acid, it is likely that the glucuronides formed in this study are conjugated at the terminal carboxylic acid. This prediction is in line with the previous finding by Samokyszyn et al. (2000) that the UGT2B7-mediated glucuronidation of ATRA and 4-oxo ATRA is directed toward the carboxyl function, whereas the 4-hydroxylated metabolite is glucuronidated almost exclusively at the hydroxyl function. It is also likely that 4-hydroxy 13*cis*RA undergoes glucuronidation. This activity would most likely occur at the hydroxyl function, as has been demonstrated for 4-hydroxy ATRA (Samokyszyn et al., 2000).

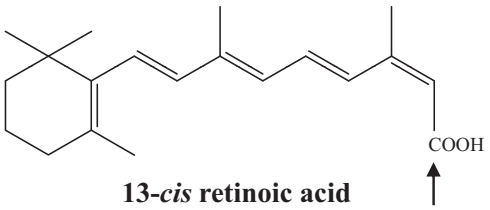

13-*cis* retinoic acid

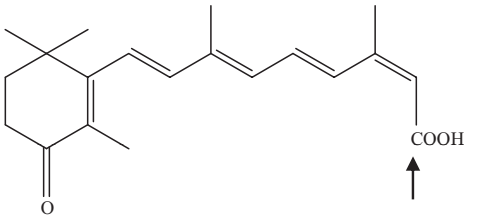

4-oxo 13-*cis* retinoic acid

FIG. 5. Structures of 13*cis*RA and 4-oxo 13*cis*RA. Arrows indicate the predicted site of glucuronidation.

However, because this metabolite is not readily available, investigations into the potential glucuronidation of 4-hydroxy 13*cis*RA could not be performed.

Despite being unable to determine the exact contribution of each of the recombinant UGT isoforms examined in this study, our data suggest that UGT1A3 has the highest rate of activity toward both substrates, as assessed by the V_{max} estimates. UGT1A3 is one of the main isoforms responsible for the glucuronidation of the majority of carboxylic acid compounds (Sakaguchi et al., 2004), supporting the hypothesis that the carboxyl function is the site of 13*cis*RA and 4-oxo 13*cis*RA glucuronidation. However, although UGT1A3 is expressed mainly in the liver, the level of expression is significantly lower than that of UGT1A1 or UGT1A9 (Ohno and Nakajin, 2009). Furthermore, because the plasma concentrations of 13*cis*RA and 4-oxo 13*cis*RA are reported to be below the K_m concentrations for the enzymes tested in this study (Veal et al., 2007), it is probable that UGT1A9 is the most important isoform in the glucuronidation of both 13*cis*RA and 4-oxo 13*cis*RA, the enzyme with the lowest K_m value for each substrate, is expressed at high levels in the liver and is also expressed in the intestine (Ohno and Nakajin, 2009). The importance of glucuronidation in the intestines is emphasized by the very high degree of glucuronidation observed with human intestinal microsomes and the high level of expression of the relevant isoforms in this tissue (Ohno and Nakajin 2009). Identification of UGT1A9 as an important isoform involved in the glucuronidation of both 13*cis*RA and 4-oxo 13*cis*RA provides a rationale for investigating the impact of UGT1A9 genetic polymorphisms on the reported variability associated with 13*cis*RA pharmacokinetics and metabolism in children with neuroblastoma (Veal et al., 2007).

Acknowledgments. We are grateful to F. Hoffman-La Roche for providing 4-oxo 13*cis*RA and 4-oxo all-*trans* retinoic acid.

References

Chen H, Fantel AG, and Juchau MR (2000) Catalysis of the 4-hydroxylation of retinoic acids by cyp3a7 in human fetal hepatic tissues. *Drug Metab Dispos* **28:**1051–1057.

Cheng Z, Radominska-Pandya A, and Tephly TR (1999) Studies on the substrate specificity of human intestinal UDP-glucuronosyltransferases 1A8 and 1A10. *Drug Metab Dispos* **27:**1165–1170.

Crespi CL and Miller VP (1999) The use of heterologously expressed drug metabolizing enzymes—state of the art and prospects for the future. *Pharmacol Ther* **84:**121–131.

Czernik PJ, Little JM, Barone GW, Raufman JP, and Radominska-Pandya A (2000) Glucuronidation of estrogens and retinoic acid and expression of UDP-glucuronosyltransferase 2B7 in human intestinal mucosa. *Drug Metab Dispos* **28:**1210–1216.

Evans TR and Kaye SB (1999) Retinoids: present role and future potential. *Br J Cancer* **80:**1–8.

Hong WK and Itri LM (1994) *The Retinoids: Biology, Chemistry, and Medicine,* Raven Press, New York.

Iwuchukwu OF and Nagar S (2010) *cis*-Resveratrol glucuronidation kinetics in human and recombinant UGT1A sources. *Xenobiotica* **40:**102–108.

Marill J, Capron CC, Idres N, and Chabot GG (2002) Human cytochrome P450s involved in the metabolism of 9-*cis*- and 13-*cis*-retinoic acids. *Biochem Pharmacol* **63:**933–943.

Matthay KK, Reynolds CP, Seeger RC, Shimada H, Adkins ES, Haas-Kogan D, Gerbing RB, London WB, and Villablanca JG (2009) Long-term results for children with high-risk neuroblastoma treated on a randomized trial of myeloablative therapy followed by 13-*cis*-retinoic acid: a Children's Oncology Group study. *J Clin Oncol* **27:**1007–1013.

Nagar S and Remmel RP (2006) Uridine diphosphoglucuronosyltransferase pharmacogenetics and cancer. *Oncogene* **25:**1659–1672.

Ohno S and Nakajin S (2009) Determination of mRNA expression of human UDP-glucuronosyltransferases and application for localization in various human tissues by real-time reverse transcriptase-polymerase chain reaction. *Drug Metab Dispos* **37:**32–40.

Peck GL and DiGiovanna JJ (1994) *The Retinoids: Biology, Chemistry, and Medicine,* Raven Press, New York.

Reynolds CP and Lemons RS (2001) Retinoid therapy of childhood cancer. *Hematol Oncol Clin North Am* **15:**867–910.

Sakaguchi K, Green M, Stock N, Reger TS, Zunic J, and King C (2004) Glucuronidation of carboxylic acid containing compounds by UDP-glucuronosyltransferase isoforms. *Arch Biochem Biophys* **424:**219–225.

Samokyszyn VM, Gall WE, Zawada G, Freyaldenhoven MA, Chen G, Mackenzie PI, Tephly TR, and Radominska-Pandya A (2000) 4-Hydroxyretinoic acid, a novel substrate for human liver microsomal UDP-glucuronosyltransferase(s) and recombinant UGT2B7. *J Biol Chem* **275:**6908–6914.

Veal GJ, Cole M, Errington J, Pearson AD, Foot AB, Whyman G, Boddy AV, and UKCCSG Pharmacology Working Group (2007) Pharmacokinetics and metabolism of 13-*cis*-retinoic acid (isotretinoin) in children with high-risk neuroblastoma—a study of the United Kingdom Children's Cancer Study Group. *Br J Cancer* **96:**424–431.

Address correspondence to: Dr. Sophie E. Rowbotham, CRUK Cambridge Research Institute, University of Cambridge, Cambridge CB2 0RE, UK. E-mail: sophie.rowbotham@cancer.org.uk